

A partitioned approach for the coupling of SPH-ALE and FE methods for transient FSI problems with incompatible time-steps

J. NUNEZ^a, Z. LI^b, J.C. MARONGIU^c, M. BRUN^d, A. COMBESURE^e

a. LaMCoS UMR 5259, Villeurbanne, France. jorge.nunez-ramirez@insa-lyon.fr

b. LMFA UMR 5509, Ecully, France

c. Andritz Hydro SAS, Villeurbanne, France

d. LGCIE, EA 4126, Villeurbanne, France

e. Professeur de la chaire AREVA-SAFRAN, LaMCoS UMR 5259, Villeurbanne, France

Résumé :

Une technique de couplage des sous-domaines garantissant la conservation d'énergie à l'interface permet de réaliser des simulations fluide-structure précises et stables. Si l'on utilise des intégrateurs temporels explicites pour réaliser ce couplage, il devient nécessaire de pouvoir intégrer chaque sous-domaine avec un pas de temps distinct afin d'éviter que les contraintes de pas de temps d'un sous-domaine soient imposées aux autres sous-domaines du calcul. Le but de cette étude est de mettre en place une méthode permettant d'intégrer chaque sous-domaine avec des pas de temps différents tout en respectant les propriétés de conservation d'énergie à l'interface

Abstract :

A previously developed interface energy-conserving coupling technique allows to carry out accurate and stable FSI simulations. In order to prevent the time-step size requirements of one domain from being inherited by the other domain, one must be able to integrate each domain with a different time-step. The purpose of this study is to implement a method allowing to integrate each domain with separate time-steps while respecting the conservation properties of the initially proposed coupling technique

Mots clefs : Interaction fluide-structure, conservation de l'énergie, couplage multi-échelle en temps

1 Introduction

An interface-energy-conserving coupling strategy for transient fluid-structure interaction was previously developed to couple Finite-Element and SPH-ALE solvers in a non-intrusive and synchronized manner [1],[2]. By imposing the interface's normal velocity continuity, the proposed coupling method ensured that neither the energy injection nor dissipation occurred at the interface, thus guaranteeing the coupling simulation's stability over time. Using different time integrators for each sub-domain (2nd

order Runge-Kutta scheme for the fluid and an explicit Newmark time integrator for the solid), the method allowed for the resolution of problems where the time steps were the same for each subdomain all while fulfilling the stability and accuracy criteria needed for successful FSI simulations. The use of explicit time integrators on both subdomains allows for a simplification in the system of equations to solve since the un-updated quantities depend exclusively on previously known quantities, excluding the need for iteration procedures to update the solid and fluid status. However, explicit integration schemes are known for their inherent instability and hence their dependability on the size of the time steps in order to procure converged results. When using the same time step on both subdomains the coupling's algorithm rapidity is dictated by the size of the smallest needed time-step which is obtained through the application of the CFL condition on both the solid and the fluid. In order to optimize the algorithm's efficiency and stability, it becomes important to be able to integrate each sub-domain with a different time-step all while respecting the zero energy condition at the interface. For this study we propose a solution for integrating each subdomain with different time-steps. When a smaller time-step is needed in the solid subdomain, we implement the incompatible time-step integration method that was devised for applications in solid mechanics by Gravouil and Combescure (GC Method) in 2001 [6] as well as that devised by Mahjoubi, Gravouil and Combescure (MGC method) in 2011 [3]. In the case where smaller time-steps are needed in the fluid, the technique used is more straightforward as the solution regarding the interface's position is given and only data needed to obtain the pressure at the interface comes from the fluid solver which is integrated with a smaller time-step.

2 An interface energy-conserving coupling strategy

2.1 Fluid pressure at solid wall

For this study, the SPH-ALE method will be used for fluid simulation. The hypothesis of a weakly compressible inviscid flow will be taken into account.

Additionally, Vila's formulation [4] of the SPH-ALE method will be expressed in a Lagrangian framework. This becomes very helpful as it allows to track in a natural way the time-evolving fluid-structure interface, which is of great importance when studying this type of phenomenon.

The truncation of the kernel function by a solid wall requires a special treatment in order to impose adequate boundary conditions that allow to solve the problem at hand. By solving a partial Riemann problem at the boundary, Marongiu [5] proposed the following expression for the pressure at the solid boundary

$$p_k = \sum_{i \in D_k} \omega_i W_{ik}^2 p_{E,ik} \quad (1)$$

where p_k stands for the fluid pressure at the solid wall element k , i is one of the fluid particles which are near to the element k , W_{ik} is the value of the kernel function at the solid wall and, finally, $p_{E,ik}$ is the elemental pressure obtained from the partial Riemann problem between the fluid particle i and the solid wall element k . Using the acoustic approximate Riemann solver, the elemental pressure $p_{E,ik}$ may be related to the fluid velocity \mathbf{v}_k at the solid wall element k by :

$$p_{E,ik} = p_i - \rho_i c_i (\mathbf{v}_k - \mathbf{v}_i) \cdot \mathbf{n}_k \quad (2)$$

Substituting (2) into (1) yields a relation between the fluid pressure at the wall element k and the fluid velocity pointing in the normal direction

$$\left(\sum_{i \in D_k} 2\omega_i \rho_i c_i W_{ik} \right) v_{fb,k} + p_k = \sum_{i \in D_k} 2\omega_i (p_i + \rho_i c_i \mathbf{v}_i \cdot \mathbf{n}_k) W_{ik} \quad (3)$$

where $v_{fb,k} \equiv \mathbf{v}_k \cdot \mathbf{n}_k$, is the fluid velocity along the normal direction at the solid boundary element k . Thanks to the latter expression, we can assemble the system of equations that relate the interface wall pressure to the velocity of the wall at both instants of the Runge-Kutta 2 (mid-point) time integrator used for the fluid subdomain.

$$\begin{cases} \mathbf{K}_{fc}^{n+\frac{1}{2}} \mathbf{v}_{fb}^{n+\frac{1}{2}} + \mathbf{\Lambda}^{n+\frac{1}{2}} = \mathbf{g}_f^{n+\frac{1}{2}} \\ \mathbf{K}_{fc}^{n+1} \mathbf{v}_{fb}^{n+1} + \mathbf{\Lambda}^{n+1} = \mathbf{g}_f^{n+1} \end{cases} \quad (4)$$

To avoid cumbersome expressions, the values of \mathbf{K}_{fc} , \mathbf{g}_f , can be obtained by consulting [1].

Equation (4) is the first of a set of three equations that are needed to solve the FSI problem with the proposed coupling method.

2.2 Finite-Element method for the solid

The finite-element method is used to discretize the solid's governing equations [12]. The semi-discrete equations for the solid sub-domain are written as

$$\mathbf{M} \mathbf{a}_s + \mathbf{f}_{int} - \mathbf{f}_{ext} = \mathbf{0} \quad (5)$$

where \mathbf{M} denotes the mass matrix, \mathbf{a}_s is the solid acceleration field, \mathbf{f}_{int} and \mathbf{f}_{ext} are the internal and external nodal forces, respectively.

Equation (5) describes the dynamical equilibrium of the solid system. Considering that at time t^n , \mathbf{a} , all variables are known, a time-integration scheme is implemented to search the value of variables at time t^{n+1} . The Newmark time-integration scheme is used to integrate the semi-discrete equations in time. Taking $\Delta t = t^{n+1} - t^n$, (5) is expressed as

$$\mathbf{M} \mathbf{a}_s^{n+1} + \mathbf{f}_{int}^{n+1} - \mathbf{f}_{ext}^{n+1} = \mathbf{0} \quad (6)$$

with

$$\begin{cases} \mathbf{u}_s^{n+1} = \mathbf{u}_s^n + \Delta t \mathbf{v}_s^n + \frac{\Delta t^2}{2} [(1 - 2\beta) \mathbf{a}_s^n + 2\beta \mathbf{a}_s^{n+1}] \\ \mathbf{v}_s^{n+1} = \mathbf{v}_s^n + \Delta t [(1 - \gamma) \mathbf{a}_s^n + \gamma \mathbf{a}_s^{n+1}] \end{cases} \quad (7)$$

where \mathbf{u}_s^{n+1} , \mathbf{v}_s^{n+1} and \mathbf{a}_s^{n+1} represent the displacement, the velocity and the acceleration fields at the next time-step t^{n+1} , with β and γ being the two coefficients of the Newmark scheme.

Finally, since a mid-point Runge-Kutta scheme is being used on the fluid for time-integration, a mid-point stage will be calculated with the Newmark integrator in order to effectively synchronize both subdomains

$$\begin{cases} \mathbf{Ma}_s^{n+\frac{1}{2}} = \mathbf{f}_{ext}^{n+\frac{1}{2}} - \mathbf{f}_{int}^{n+\frac{1}{2}} \\ \mathbf{Ma}_s^{n+1} = \mathbf{f}_{ext}^{n+1} - \mathbf{f}_{int}^{n+1} \end{cases} \quad (8)$$

In the case of large deformations for the solid structure or non-linear material properties, the expression of the internal nodal forces becomes more complex than for the linear case. In order to avoid an iterating process that hampers the resolution procedure by making it more time-consuming, the explicit Newmark time-integrator is chosen by setting $\beta = 0$ and $\gamma = 0.5$.

We now proceed to combine the explicit Newmark scheme (obtained from (7) when $\beta = 0$ and $\gamma = 0.5$), with (8) to yield [1],[2].

$$\begin{cases} \mathbf{K}_{sc}^{n+\frac{1}{2}} \mathbf{v}_s^{n+\frac{1}{2}} + \mathbf{L}_p^{n+\frac{1}{2}} \mathbf{\Lambda}^{n+\frac{1}{2}} = \mathbf{g}_s^{n+\frac{1}{2}} \\ \mathbf{K}_{sc}^{n+1} \mathbf{v}_s^{n+1} + \mathbf{L}_p^{n+1} \mathbf{\Lambda}^{n+1} = \mathbf{g}_s^{n+1} \end{cases} \quad (9)$$

where \mathbf{L}_p is a geometric operator that relates the interface pressure field $\mathbf{\Lambda}$ with the external nodal forces associated with the fluid pressure loading $\mathbf{f}_{ext,f}$. In addition, \mathbf{K}_{sc} and \mathbf{g}_s are two matrices which take into account the internal forces and kinematic quantities from previous iterations. Once again, for the sake of brevity the expressions of these operators will be omitted. They can be obtained in [1].

2.3 Coupling strategy

When coupling two continua with different time integrators, the numerical stability and the minimal order of accuracy can be preserved as long as the interface energy is nil during the numerical simulation [6].

The following equation defines the increment of the interface energy over the time interval $t \in [t^n, t^{n+1}]$ as

$$\Delta \mathcal{W}_I = \int_{t^n}^{t^{n+1}} \int_{\Gamma_I} \mathbf{n}_s \cdot (-p_s \mathbf{I}) \cdot \mathbf{v}_s + \mathbf{n}_f \cdot (-p_f \mathbf{I}) \cdot \mathbf{v}_f \, d\Gamma \, dt \quad (10)$$

where $\Gamma_I(\mathbf{x}, t)$ denotes the moving fluid-solid interface, $\mathbf{n}_s(\mathbf{x}, t)$ and $\mathbf{n}_f(\mathbf{x}, t)$ are the outward-pointing vectors for the solid and the fluid, respectively. The external forces exerted on the solid and fluid subdomains are thus expressed as $\mathbf{n}_s(\mathbf{x}, t) \cdot [-p_s(\mathbf{x}, t) \mathbf{I}]$ and $\mathbf{n}_f(\mathbf{x}, t) \cdot [-p_f(\mathbf{x}, t) \mathbf{I}]$. Assuming the pressure to be homogeneous over each elemental surface, it has been shown in [1] that the discrete form of the algorithmic interface-energy can be written as

$$\Delta \mathcal{W}_I^d = \sum_k^{N_k} \Delta t s_k(t) \overline{p_k(t) s_k(t)} \overline{\mathbf{n}_k(t) \cdot [\mathbf{v}_s(\mathbf{x}_k, t) - \mathbf{v}_f(\mathbf{x}_k, t)]} \quad (11)$$

Hence, to keep a zero algorithmic energy (11) at the inter- face, one can simply impose a velocity constraint condition at each interface element

$$\overline{\mathbf{n}_k(t) \cdot [\mathbf{v}_s(\mathbf{x}_k, t) - \mathbf{v}_f(\mathbf{x}_k, t)]} = 0 \quad (12)$$

The above expression is the key point of this coupling method. Instead of imposing the velocity continuity at each instant, we ensure the equality of mean normal velocity over each time-step. This guarantees

rigorously the zero interface energy condition over each time interval and thus for the whole period of the simulation.

In order to adapt the energy conserving expression to the previously presented numerical integrators, condition (12) is imposed at $t^{n+\frac{1}{2}}$ and the next time-step t^{n+1} as

$$\begin{cases} \mathbf{n}_k^{n+\frac{1}{2}} \cdot [\mathbf{v}_s(\mathbf{x}_k^{n+\frac{1}{2}}) - \mathbf{v}_f(\mathbf{x}_k^{n+\frac{1}{2}})] = 0 \\ \mathbf{n}_k^{n+1} \cdot [\mathbf{v}_s(\mathbf{x}_k^{n+1}) - \mathbf{v}_f(\mathbf{x}_k^{n+1})] = 0 \end{cases} \quad (13)$$

3 Incompatible time step implementation

3.1 Smaller time scale in the solid

Let us consider first the case where the smaller time steps are present on the solid subdomain. As presented before, the solid will be integrated with a conventional Newmark scheme using the explicit central difference scheme. As a first hypothesis, let's consider that the solid domain's time-step is a multiple of that of the fluid subdomain.

$$\Delta t_f = m \Delta t_s, \quad m \in \mathbb{N}^* \quad (14)$$

For this study we will implement the incompatible time-step integration method that was devised by Mahjoubi, Gravouil and Combescure (MGC method) in 2011 [3]. This method relies on the use of a constant Lagrange multiplier representing the interface pressure for the duration of the whole macro time-step to integrate the micro time steps. This method was developed to be used with integrators of the Newmark family using increments of velocity at the interface. For the current study this method was adapted to what was presented in the previous sections, which represented a simplification of the system's matrices.

Next, let's consider j as one of the micro substeps present in the interval $I \in [1, m]$. Applying this to the conservation equation presented previously gives

$$\overline{\mathbf{n}_k(t) \cdot [\mathbf{v}_s(\mathbf{x}_k, t) - \mathbf{v}_f(\mathbf{x}_k, t)] s_k(t)} = \frac{1}{m \Delta t_s} \sum_{j=0}^{m-1} \int_{t^j}^{t^{j+1}} \mathbf{n}_k(t) \cdot \mathbf{v}_s(\mathbf{x}_k, t) s_k(t) dt - \frac{1}{\Delta t_f} \int_{t^n}^{t^{n+1}} \mathbf{n}_k(t) \cdot \mathbf{v}_f(\mathbf{x}_k, t) s_k(t) dt \quad (15)$$

for this integration scheme, we will first consider that the mean pressure at each micro-timestep \bar{p}_s^j is equal to the mean pressure along the macro-timestep \bar{p}_f . As done previously, we impose a strong equilibrium condition for the pressure at the interface. Both of these assumptions yield

$$\bar{p}_k = \bar{p}_f = \bar{\bar{p}}_s \quad (16)$$

We choose then a unique pressure \bar{p} to integrate both domains along the micro and macro time steps. This is the fundamental hypothesis behind the MGC method because it is a method that links the

domains at the macro (larger) time scale. Additionally, we consider that the normals and wall element surfaces used to solve interface problem at the interface remain constant throughout the whole macro time-step, i.e.

$$\mathbf{n}_k^j = \mathbf{n}_k^n = \mathbf{n}_k \quad \text{and} \quad s_k(t^j) = s_k(t^n) = s_k \quad (17)$$

Hence the interface operators become

$$\mathbf{L}_s^j = \mathbf{L}_s^n = \mathbf{L}_s \quad \text{and} \quad \mathbf{L}_p^j = \mathbf{L}_p^n = \mathbf{L}_p \quad (18)$$

Although at a first glance these assumptions might come off as strong approximations to make, the fact that the present technique is aimed at coupling fast dynamics FSI problems, where the time-step will be relatively small for both subdomains, makes it safer to assume that the pressure and the interface operators will vary only slightly in between iterations.

An alternative against having to make these assumptions, would be to use a coupling technique that links the subdomains at the micro-time scale such as the GC method. The GC method is similar to the MGC method, only that the pressure or Lagrange multiplier must be obtained at every micro-iteration by solving the interface problem at the micro-time scale. This method comes in handy when solving FSI problems involving strong non-linearities. The drawback comes from the fact that information needs to be exchanged between codes at each micro time-step. This method was implemented as well for the proposed coupling method, but for the sake of brevity we will only focus on giving an overview of the MGC method in this paper. The reader can find more about the GC method in [6].

From [1] we have

$$\overline{\mathbf{n}_k \cdot \mathbf{v}_s(\mathbf{x}_k)} s_k - \overline{\mathbf{n}_k \cdot \mathbf{v}_f(\mathbf{x}_k)} s_k = 0 \quad (19)$$

In matricial terms, we get the following system that needs solve for at each time step :

$$\frac{1}{m} \mathbf{n}_k s_k \sum_{j=0}^{m-1} \frac{[\mathbf{v}_s(\mathbf{x}_k^{j+1}) + \mathbf{v}_s(\mathbf{x}_k^j)]}{2} - \mathbf{n}_k \cdot \frac{[\mathbf{v}_f(\mathbf{x}_k^{n+1}) + \mathbf{v}_f(\mathbf{x}_k^n)]}{2} s_k = 0 \quad (20)$$

The system needed to update the solid status from t^n to t^{n+1} becomes slightly more complex than before, as we now have to solve m times the system that allows to update from t^j to t^{j+1} all the solid kinematic quantities with the inclusion of a trailing term that takes into account terms from the previous micro time-step t^{j-1} . The great advantage comes from the fact that now each subdomain can be integrated using an optimal choice for their respective time-steps.

When using the MGC method, the calculation of the Stenov-Poincare H requires now the resolution of a linear system of equations. In order to avoid adding more cumbersome expressions to this review, the reader can learn more about how to obtain this operator by consulting [3].

Finally, Figure (1) presents the coupling procedure implemented for the the integration of both the fluid and the solid subdomains from t^n to t^{n+1} . Notice that the interface problem is solved at the macro-scale but in order to get the necessary information from the solid wall (position and normal vectors) and to get the interface operator H, iterations through the micro-steps must take place.

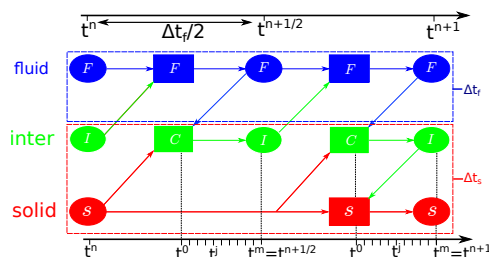


FIGURE 1 – Overview of the coupling procedure when the solid uses a smaller time-step than the fluid, i.e. $\Delta t_f = m\Delta t_s$

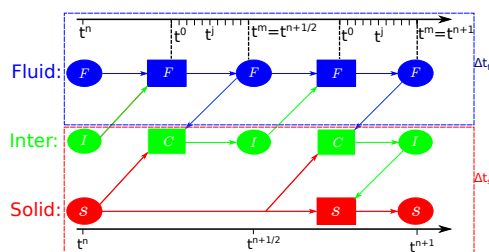


FIGURE 2 – Overview of the coupling procedure when the fluid uses a smaller time-step than the solid, i.e. $\Delta t_s = m\Delta t_f$ and information from the interface comes only at the beginning of each macro-time step $t^0 = t^n$

3.2 Smaller time scale in the fluid

Despite the faster propagation of waves through solid continua in general for the phenomena we are considering, cases where a smaller particle size might be needed for the coupled calculation could require the implementation of smaller time steps within the fluid. In this cases, the integration of the domain possessing the smaller time step becomes much more straightforward as the position of the interface is given by the calculation from the solid's and coupler's side which is done with a bigger time-step.

For the fluid's subdomain integration, 2^{nd} order Runge Kutta (mid-point version) had been implemented when previously integrating with a larger time step. In order to keep the the order of accuracy and stability of this integrating scheme during the integration through the micro time scale the same integration scheme will be used as a way of going from micro-step j to micro step $j + 1$.

Figure (2) shows how the integration procedure is carried out. The solid and the coupler make use of a larger time step ($\Delta t_s = m\Delta t_f$) for the determination of the necessary operators and kinematic quantities, which are then transferred to the fluid, to make its own integration along the micro-time scale.

For the current implementation of micro time steps in the fluid subdomain, the position of the wall is given at the beginning of the macro time-step only. This approach allowed for accurate results when compared to results when both subdomains where integrated with the same time step.

In order to increase the accuracy of the method, one can give an estimate of the position of the wall (21) using the wall kinematic quantities known at $j = 0$ (here noted as U_{fb}^0). Nevertheless, this approach would require a bigger volume of data to transfer, since the acceleration of the wall will be needed to calculate the estimated position and velocity of the wall.

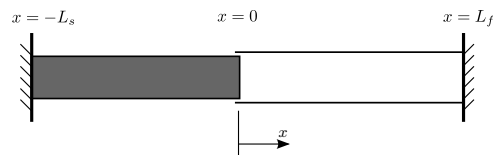


FIGURE 3 – 1D linear beam coupled with a column of water ? propagation of shock wave across the fluid ?structure interface

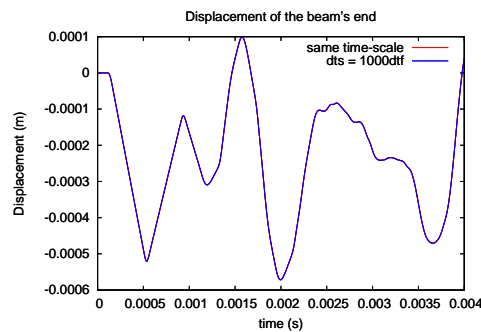


FIGURE 4 – 1D propagation of shock wave across the interface - Comparison between the results obtained when integrating with same and different time-steps in both domains

$$\tilde{\mathbf{u}}_{fb}^j = \mathbf{u}_{fb}^0 + j\Delta t_f \mathbf{v}_{fb}^0 + \frac{(j\Delta t_f)^2}{2} \mathbf{a}_{fb}^0 \quad (21)$$

Up until now, this technique has worked when used for solving 1D cases where the fluid structure interface is much smaller when compared to the size of the whole problem. In the following section, some examples will be presented where a comparison is drawn between coupling calculations done with the same time-steps and those done using different time steps for each subdomain.

4 Numerical Results

4.1 1-D propagation of shock wave across the fluid-structure interface

For the first test case we couple cantilever 1D linear beam to a water tube inside which a strong pressure gradient induces a shock wave across the interface(Figure 3)

The initial length of the beam is $L_s^0 = 1$ m, its initial solid density $\rho_s^0 = 2700$ kg/m³, and its initial section area $A_s^0 = 0.01$ m². The Young's modulus is $E_s = 67.5$ GPa. The solid beam is discretized with 100 linear truss finite-elements. The tube has also a length of $L_f^0 = 1$ m but contains ten times as many particles as the beam has elements. A uniform pressure step of 20 MPa is imposed at the time $t = 0$ s in the fluid cavity. For this test case, we use a time step of $\Delta t_s = 10^{-6}$ s for the solid and $\Delta t_f = 10^{-9}$ s for the fluid. Hence a ratio m of 1000 exists between both domains.

Figure (4) shows the comparison between the results of the simulation described above and another one in which both subdomains are clumsily integrated with the same time-step, i.e. $\Delta t_f = \Delta t_s = 10^{-9}$ s. The results show good agreement with respect to the same case-study using the same time-step.

4.2 2-D hydrostatic water on a linear elastic plate

Next, we consider a 2-D test case in which we couple a linear elastic plate with a column of water which is initially in hydrostatic equilibrium. Figure 5 shows the configuration of this test case : a rigid water reservoir has a geometrically linear elastic bottom which is clamped at the two sides, a pressure gradient of water is present due to the gravity effect and at the free surface the fluid pressure equals zero. The simulation parameters are given in [2].

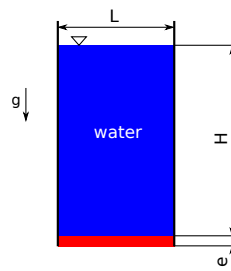


FIGURE 5 – 2-D hydrostatic water interacting with a linear elastic plate.

This test case is aimed at assessing the accuracy of the MGC method in 2D. As stated in [2] the fluid and the solid domains are discretized in a similar manner. The speed of sound being roughly five times larger in the structure than in the fluid, a time-step used to integrate the fluid of $\Delta t_f = 5 \times 10^{-7}$ s will be used while that of the solid will be twenty times smaller.

The results of the simulation are given in Figure 6. Once again, good agreement exists between the results obtained by clumsily integrating both domains with the same time-step and those obtained through the use of the MGC technique.

4.3 Breaking dam flow on an elastic wall

Next, we consider another 2D test case of fluid-structure interaction problem, of which the initial configuration is shown in Figure 7. As one can observe, in a rigid wall container a column of water is initially located at the left side of a container, which is in hydrostatic equilibrium. An elastic wall is clamped placed to the right at the middle of the container. Once again the geometric and discretization parameters are given in [2]. The material properties of the solid are such that the initial solid density is $\rho_s^0 = 2500 \text{ kg/m}^3$, the Young's modulus is $E_s = 10^6 \text{ Pa}$ and the Poisson's ratio will be taken to be $\nu = 0$. As Walhorn et al. [8] did, we applied a linear elasticity model which gives a linear relationship

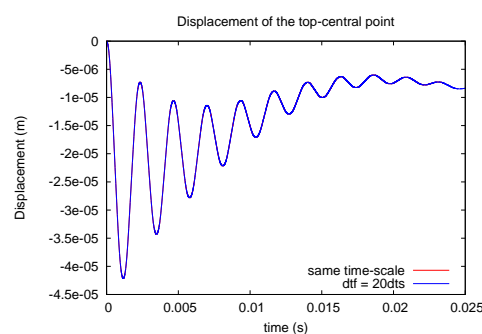


FIGURE 6 – 2-D hydrostatic water on a linear elastic plate - Comparison between the results obtained when integrating with same and different time-steps in both domains

between the Green strain tensor \mathbf{E} and the second Piola-Kirchhoff stress tensor \mathbf{S} .

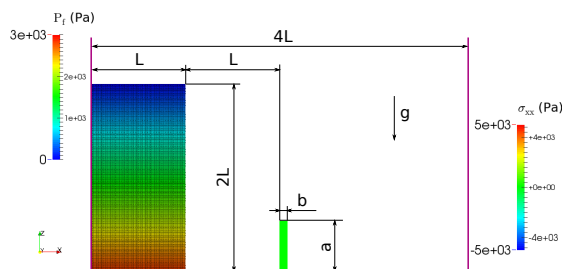


FIGURE 7 – Initial configuration of the test case : breaking dam flow on an elastic wall.

This test case will aim at assessing how the proposed technique responds to the presence of strong geometrical non-linearities. Once again, due to the same spatial discretization used on both domains, we will use a time-step of $\Delta t_f = 2 \times 10^{-5}$ s for the fluid while the structure will have a time-step that is 10 times smaller. Additionally, we will make use of the GC coupling technique[6], which is much more suited for coupling problems involving large deformations like this one than the MGC technique featured previously. The GC technique imposes velocity continuity at the micro-scale by doing a linear interpolation of the velocity coming from the domain integrated with the larger time-step. Figure 8 shows the result of the simulation for $t = 0.30$ s.

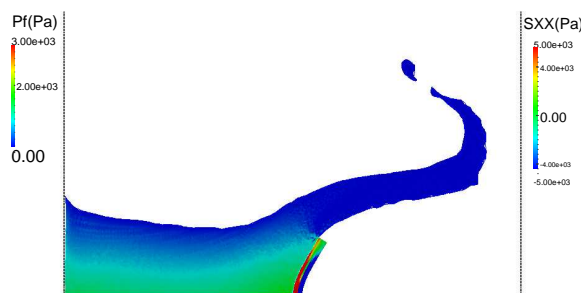


FIGURE 8 – Breaking dam flow on an elastic wall - result of the simulation for $t = 0.30$ s

Finally we compare in Figure 9 the results of the simulation with the results obtained by other authors [8],[9]. A comparison is also made between the current results and those obtained previously when another solid solver was used. In fact, the coupling strategy initially made exclusive use of Code Aster, a finite-element implicit/explicit code developed by EDF (Electricité de France). As of now, the SPH-ALE code (ASPHODEL) can be coupled to the Europlexus code which is developed by the CEA (Commissariat à l'Énergie Atomique) which is an explicit code focusing on the simulation of fast dynamics phenomena.

As presented in [2], there is still a discrepancy between the results obtained in [8] and those obtained through the use of the present method. However the results obtained by [9] come quite close to what was obtained with the proposed method, especially for the coupling done with the Europlexus software. Good agreement between the results obtained when integrating with same and different time-steps is also found, despite the large displacements undergone by the structure. The latter aspect justifies the implementation of the GC algorithm for this case-study as the velocity equilibrium condition is verified at each micro time-step.

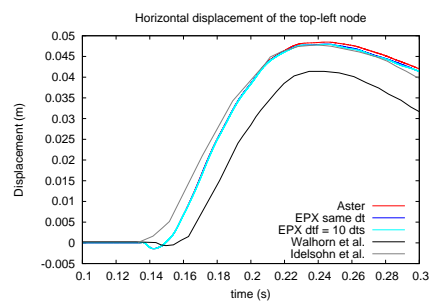


FIGURE 9 – Displacement of the top left node of the structure until $t = 0.3$ s- result comparison

5 Conclusion

A previously developed interface energy-conserving coupling technique allows to carry out accurate and stable FSI simulations. If explicit time integrators on both physical domains are used, the linear systems involved become much simpler to solve, however dependability on the time-step size becomes a major drawback. In order to prevent the time-step size requirements of one domain from being inherited by the other domain, one must be able to integrate each domain with a different time-step. This objective was accomplished in different ways for both domains. When the smaller time-step is needed for the solid subdomain, the use of techniques coming from the coupling of solid subdomains allows to accomplish this successfully. For the fluid, the technique used is more straightforward. Numerical case-studies allowed to test the implemented techniques and gave satisfactory results. Future work will focus on adapting this techniques in order to increase its robustness and be able to study complex FSI phenomena.

Acknowledgement

Part of the research leading to these results has received funding from the European Community's Seventh Framework Programme (FP7 / 2007-2013) under Grant Agreement 608393 "PREDHYMA"

Références

- [1] Zhe, L. I. (2014). Développement d'une méthode de simulation de couplage fluide-structure à l'aide de la méthode SPH (Doctoral dissertation, Ecole Centrale de Lyon).
- [2] Li, Z., Leduc, J., Nunez-Ramirez, J., Combescure, A., Marongiu, J. C. (2015). A non-intrusive partitioned approach to couple smoothed particle hydrodynamics and finite element methods for transient fluid-structure interaction problems with large interface motion. *Computational Mechanics*, 55(4), 697-718.
- [3] N. Mahjoubi, A. Gravouil, A. Combescure, N. Greffet, A monolithic energy conserving method to couple heterogeneous time integrators with incompatible time steps in structural dynamics, *Computer Methods in Applied Mechanics and Engineering* (2011) 1069 – 1086.
- [4] J. P. Vila, On particle weighted methods and smooth particle hydrodynamics, *Mathematical models and methods in applied sciences* 9.
- [5] J. C. Marongiu, Méthode numérique lagrangienne pour la simulation d'écoulements à surface libre - Application aux turbines Pelton, Ph.D. thesis, École Centrale de Lyon (2007).

- [6] A. Combescure, A. Gravouil, A numerical scheme to couple subdomains with different time-steps for predominantly linear transient analysis, *Computer Methods in Applied Mechanics and Engineering* 191 (2002) 1129 – 1157.
- [7] Brun, M., Batti, A., Combescure, A., Gravouil, A. (2014). External coupling software based on macro-and micro-time scales for explicit/implicit multi-time-step co-computations in structural dynamics. *Finite Elements in Analysis and Design*, 86, 101-119.
- [8] Walhorn, E., Kölke, A., Hübner, B., Dinkler, D. (2005). Fluid-structure coupling within a monolithic model involving free surface flows. *Computers and structures*, 83(25), 2100-2111.
- [9] Idelsohn, S. R., Marti, J., Limache, A., Oñate, E. (2008). Unified Lagrangian formulation for elastic solids and incompressible fluids : application to fluid-structure interaction problems via the PFEM. *Computer Methods in Applied Mechanics and Engineering*, 197(19), 1762-1776.
- [10] A. Prakash, K. D. Hjelmstad, A FETI-based multi-time-step coupling method for Newmark schemes in structural dynamics, *International Journal for Numerical Methods in Engineering* 61 (2004) 2183 – 2204.
- [11] J. C. Marongiu, F. Leboeuf, J. Caro, E. Parkinson, Free surface flows simulations in Pelton turbines using an hybrid SPH-ALE method, *Journal of Hydraulic Research* 48 (2010) 40 – 49.
- [12] T. Belytschko, W. K. Liu, B. Moran, *Nonlinear Finite Elements for Continua and Structures*, John Wiley & Sons, Ltd, 2000.